(ANPA Conference 2024)
ISSN: 2392-473X(Print), 2738-9537 (Online)

Research Article ©Nepal Physical Society
DOI: https://doi.org/10.3126/jnphyssoc.v10i1.72826

First Principles Study of Undoped and Halogen Doped ZnO Monolayer

Dipak Oli, Ravi Kiran Neupane, Om Shree Rijal, Pitamber Shrestha, Shriram Sharma, Leela Pradhan Joshi, and Rajendra Parajuli[a)]

Department of Physics, Amrit Campus, Tribhuvan University

[a)]*Corresponding author:rajendra.parajuli@ac.tu.edu.np*

Abstract. This study reports the structural, electronic, and magnetic properties of undoped and halogen (F, Cl, and Br) doped ZnO monolayers ($3 \times 3 \times 1$) by replacing one Zn-atom. Using spin polarized Density Functional Theory (DFT) in VASP code and a projected augmented wave basis set, we employed GGA-PBE and PBE+U exchange correlation functionals. The band gap of pristine ZnO was measured to be 1.67 eV and 2.61 eV for PBE and PBE+U, respectively, whereas band gap decreased significantly upon addition of halogen atom. Likewise, doped ZnO shows semimetallic behavior, whereas undoped ZnO exhibits semiconducting behaviour. Further, the magnetic moments of about 1 μB for Cl and Br-doped ZnO, and 1.02 μB & 2.98 μB for F-ZnO utilizing PBE and PBE+U functionals, respectively were observed. These findings suggest that halogen-doped ZnO might carry huge potential for next-generation spintronic nanodevices.

Received: August 25, 2024; **Revised**: October 5, 2024; **Accepted**: October 29, 2024

Keywords: DFT ; Doping; Halogen; Monolayer ; Electronic properties; Magnetic Properties

INTRODUCTION

As compared to conventional 3D semiconductors, two-dimensional (2D) materials [1] with ultrathin thickness enable for higher integration densities and have demonstrated remarkable optical, electrical, and optoelectronic capabilities [2, 3]. Also, two-dimensional materials are well positioned to address the difficulties and improve the performance, efficiency, durability, and thus sustainability of electric cars in this century and beyond [4]. These properties promote the study of 2D materials for use in next-generation optoelectronics and electronics [5], such as light-emitting diodes (LEDs) [6], modulators [7], photodetectors [8], and transistors [9]. Further, a lot of attention has been drawn to recent advancements in the field of two-dimensional (2D) van der Waals (vdW) [10] materials because of potential uses in the upcoming generation of complementary metal-oxide semiconductor (CMOS) [11] technology [12]. Among various 2D materials, zinc oxide is one of the extensively studied semiconducting materials due to its high energy band gap of 3.37 eV and high binding energy of 60 meV [13–15]. Two-dimensional ZnO with honeycomb crystal structure has already been synthesized and has its excellent electronic, thermal and optical characteristics [16]. Such behavior of that compound carries a huge potential in the fields of solar cells, LED, lasers, gas sensing and many more [17, 18]. In particular, ZnO nanosheets' chemical characteristics and performance are mostly determined by their nano-structuring, which is modulating and controllable [19].

It is almost impossible to obtain a pure material devoid of impurities in the real world, impurities are typically introduced into materials in order to subtly enhance their numerous physical and chemical properties. Different properties of the nanomaterials can be tuned by adding the impurities in the compounds. However, controlled doping of the materials is crucial for device application [20–22]. To obtain the desired qualities, it could be helpful to add the right impurities in a right proportion to the compounds. One of the effective techniques to enhance the physical properties of the compound is doping. Doping is the intentional insertion of the foreign elements or impurities to the compound, which can be performed in two ways; viz, n-type and p-type doping. This work examines n-type doping using halogen atom in ZnO monolayer. Halogen are the highly reactive non-metal due to their high effective nuclear charge and strong electronegativity. Furthermore, the introduction of halo-

gen impurities into two-dimensional materials currently opens up an inconceivable research area. Halogen doping has a significant impact on the mechanical, electrical, sensing, electrochemical, and electrical properties of 2D systems like graphene and Transition Metal Dichalcogenides (TMDs) [23]. Likewise, adding halogens to 2D materials can greatly increase their capacity for adsorption [24]. It is found that doping of SnO_2 rutile [25] and Cu_2O [26] with halogens atom has been greatly enhanced their electrical conductivity. Halogen doping has a significant impact on the mechanical, electrical, sensing, electrochemical, and electrical properties of 2D systems like graphene and TMDs [27].

To optimize the performance of 2D materials, a thorough comprehension and accurate manipulation of the flaws are essential. Undoped ZnO monolayers and doped with many elements ZnO monolayers have been studied extensively, both experimentally and theoretically. So, in order to comprehend how halogen impurities affect the different properties and their applications in device design, we investigate the aforementioned properties of undoped and F, Cl, and Br doped ZnO using spin polarized DFT approach with the VASP [28] computational tool.

COMPUTATIONAL DETAILS

First-principles calculation based on DFT [29] with the plane-wave pseudo-potential method was performed as implemented in the Vienna Ab-initio Simulation Package (VASP) [28] computational tool. In order to compare and ensure the validity of our results, we have employed two different exchange correlation functional: Generalized gradient approximation (GGA) in the Perdew Burke Ernzerhof (PBE) [30] and PBE+U functional [31]. GGA-PBE approximation approximates the maximum possible results of the system. Moreover, we employed PBE+U functional to account the strong electron correlation of ZnO. Herein, Herein, ZnO have wide band energy gap between valence band and the conduction band, and for such a system, Hubbard's U potential should be used to obtain the closest results. Several previous reports have employed U potentials of 10 eV and 7 eV for Zn and O, respectively. Sheetz R M et al. [32] have used the U value of 10.5 eV and 7 eV for Zn and O atoms, respectively and found the band gap of 3.72 eV. Similarly, Ma X et al. [33] have used the U potential of 10 eV and 7 eV and they have claimed that these value is optimal value to find the appropriate band energy of the ZnO. Wu H-C et al. [34] have used the DFT+U_d+U_p method, in which the U_d value for Zn-3d and the U_p value for O-2p orbitals were set at 10 and 7 eV, respectively. Additionally, in one of the reported reviews [35], it has been concluded that the inclusion of these values of U has effectively produced the accurate band gap. Based on these published paper, we have opted the U value for Zn and O are 10 eV and 7 eV. Also, the band gap value of ZnO and halogen doped ZnO was corrected, and system energy was optimized using the PBE+U technique [36]. We used the PAW potential in the pseudopotential component to address the effect of nuclear and inner-core electrons. Using plane waves with a 360 eV kinetic energy cutoff, the valance electron ($3d^{10}$ $4s^2$ for Zn, $2s^2$ $2p^4$ for O, $2s^2$ $2p^5$ for F, $3s^2$ $3p^5$ for Cl, and $4s^2$ $4p^5$ for Br) wave functions are expanded. Herein, structural, electronic, and magnetic properties of undoped and halogen doped ZnO is studied. For all the computation, the Monkhorst–Pack method Brillouin zone is sampled using an $8 \times 8 \times 1$ k-point grid for relaxation and Scf calculation of the systems. However, DoS calculation is done by employing dense Kpoint mesh of $24 \times 24 \times 1$ and band calculations were performed by using high symmetric points (Γ-M-K-Γ). The overall energy shift on each atom for geometry relaxation is less than 10^{-6} eV. Additionally, Vaspkit [37, 38] is used to extract the required output by using raw outputs. Lastly, VESTA software [39, 40] is used to visualize the atomic structure of the compound, to doped the system and to get the Poscar file.

TABLE I. Optimized lattice parameters and bond lengths of undoped and Halogen doped ZnO monolayer obtained by using PBE and PBE+U functional.

		Lattice Parameters (Å)			Bond length(Å)			
Systems	Method	a	b	c	Zn-O	F-O	Cl-O	Br-O
ZnO	PBE	9.88	9.88	4.54	1.91	-	-	-
	PBE+U	9.20	9.20	4.54	1.91	-	-	-
F-ZnO	PBE	9.70	9.70	4.05	1.89	2.01	-	-
	PBE+U	9.27	9.27	3.94	1.75	2.18	-	-
Cl-ZnO	PBE	9.82	9.82	4.31	1.85	-	2.08	-
	PBE+U	9.29	9.29	4.26	1.74	-	2.08	-
Br-ZnO	PBE	9.79	9.79	4.52	1.87	-	-	1.94
	PBE+U	9.43	9.43	5.31	1.75	-	-	2.12

RESULTS AND DISCUSSION

Structural Properties

Initially, we obtained the unit cell of hexagonal ZnO (space group $P6_3mc$) from material projects. The unit cell is then changed to $3\times$ $3\times$ 1 super cell using VESTA software. The hexagonal structure of $3\times$ $3\times$ 1 monolayer of ZnO is shown in figure 1. Zinc oxide (ZnO) consists of an equal ratio of zinc (Zn) and oxygen (O) atoms. The resulting structure is then relaxed with narrow Gaussian smearing of 0.1, an ISIF value of 3, and a cut-off energy of 360 eV. After obtaining the relaxed structure, one Zn atom is substituted with a halogen atom. We optimized the system after doping the halogen atom to obtain the

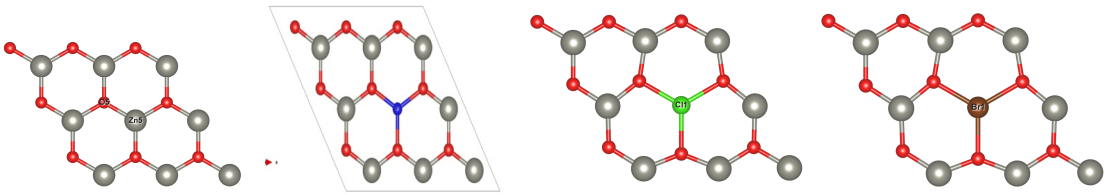

FIGURE 1. Top view of optimized structure of: Pristine ZnO, F-doped ZnO, Cl-doped ZnO and Br-doped ZnO, where brown, red, blue, green and dark brown color ball represents Zn, O, F, Cl & Br atoms, repectively

relaxed configurations of halogen-doped ZnO. Upon relaxation, we found the ground state energies for PBE and PBE+U functional to be -23.01 eV and -21.23 eV for F-ZnO, -31.23 eV and -23.31 eV for Cl-ZnO, and -37.21 eV and -33.12 eV for Br-ZnO. We further investigated the structural properties of undoped and halogen-doped ZnO (F, Cl, and Br) by analyzing the bond lengths between the nearest atoms and examining the lattice parameters. Figure 1 illustrates the top view of optimized and stable structure of Pristine, F-ZnO, Cl-ZnO, and Br-ZnO respectively.

Different lattice parameters and bond lengths of undoped and halogen doped ZnO are presented in Table I. Bond length of Zn-O for ZnO monolayer is found to be 1.91(Å) while applying PBE and PBE+U functional, which is almost similar to the previous studies [41, 42]. However, bond length between Zn-O gets decreased to be 1.89 and 1.79(Å) for F-ZnO, 1.85 and 1.74(Å) for Cl-ZnO, and 1.87(Å) and 1.75(Å) for Br-ZnO, while using PBE and PBE+U functional respectively. Similarly, the halogen atom form bond with oxygen and their corresponding bond length are 2.01 and 2.18(Å) for F-ZnO, 2.08 and 2.08(Å) for Cl-ZnO and 1.94 and 2.12(Å) for Br-ZnO while applying PBE and PBE+U functional, respectively. On the other hands, the lattice parameters of halogen doped ZnO is found comparatively less than pristine ZnO.

Electronic Properties

The electronic property is one of the widely studied properties of 2D materials, as it is very useful for device design. Generally, band structure, density of states (DoS), and projected density of states (PDoS) are computed to study the electronic behavior of the materials. Figure 2 disclose the information about the band energy and DoS of undoped and halogen doped ZnO, which is obtained by employing PBE, and PBE+U functional respectively. The vertical green dash line indicates the high symmetric points, whereas the horizontal blue dash line represents the Fermi level. For undoped ZnO , when the PBE functional is used, a band gap of 1.67 eV is obtained, which is less than the actual band gap of 3.37 eV because of the well known shortcoming of the PBE functional. In order to overcome this error, we employed PBE+U functional. On applying the suitable potential, more accurate band gap can be calculated as it accounts the 3d-orbitals of the compound. Herein, potential of 10 eV and 7 eV is used for Zn and O atom respectively. While applying these potential, a band gap of 2.61 eV is obtained that is closer to the previous study [32–35]. On the other hand, when one Zn-atom is replaced by F-atom, some of the band are seen near the Fermi level, while applying PBE functional with a narrow band gap of 0.01 eV. Similarly, a wide band gap of 1.14 eV is found when PBE+U is used. Nonetheless, on studying the spin up and spin down bands, we obtained the asymmetric nature in both the band. However, the different scenario is seen when Chlorine and Bromine atom are placed in place of Zn in ZnO. Figure 2 (c) represent the band energy and 2 (g) DoS of Cl-ZnO. Both of them agree with each other. When Cl-atom is doped in the ZnO, some of the band are seen around Fermi level, while applying the PBE and PBE+U functionals. Also, band gap obtained, while using both the functional are almost 0 eV. Moreover, Figure 2(d) and 2 (h) shows the Band and DoS of Br-ZnO. Both of them vividly agree with one another. We found the band gap for both the functional was about 0 eV after doping with Br-atom in ZnO monolayer. Based on the findings, we discovered that adding a halogen atom in place of the Zn atom increases the system's conductivity. Further, on studying the DoS of all system, we obtained that ZnO which is semiconductor that behaves like a magnetic material after doping with halogen atom.

Magnetic Properties

Ferromagnetic semiconductors are simple to integrate into semiconductor systems by appropriate doping of the foreign elements and their magnetic materials are considered as beneficial in the field of spintronics [43, 44]. In addition to inherent magnetic materials, dilute magnetic semiconductors (DMSs) [43] in which doping of hole impurities induces magnetism, have also been the subject of research interest. In this study, density of states (DoS) and partial density of states (PDoS) is analyzed to study the magnetic properties of the undoped and halogen doped ZnO. Figure 3 and 4 depicts the DoS and PDoS of

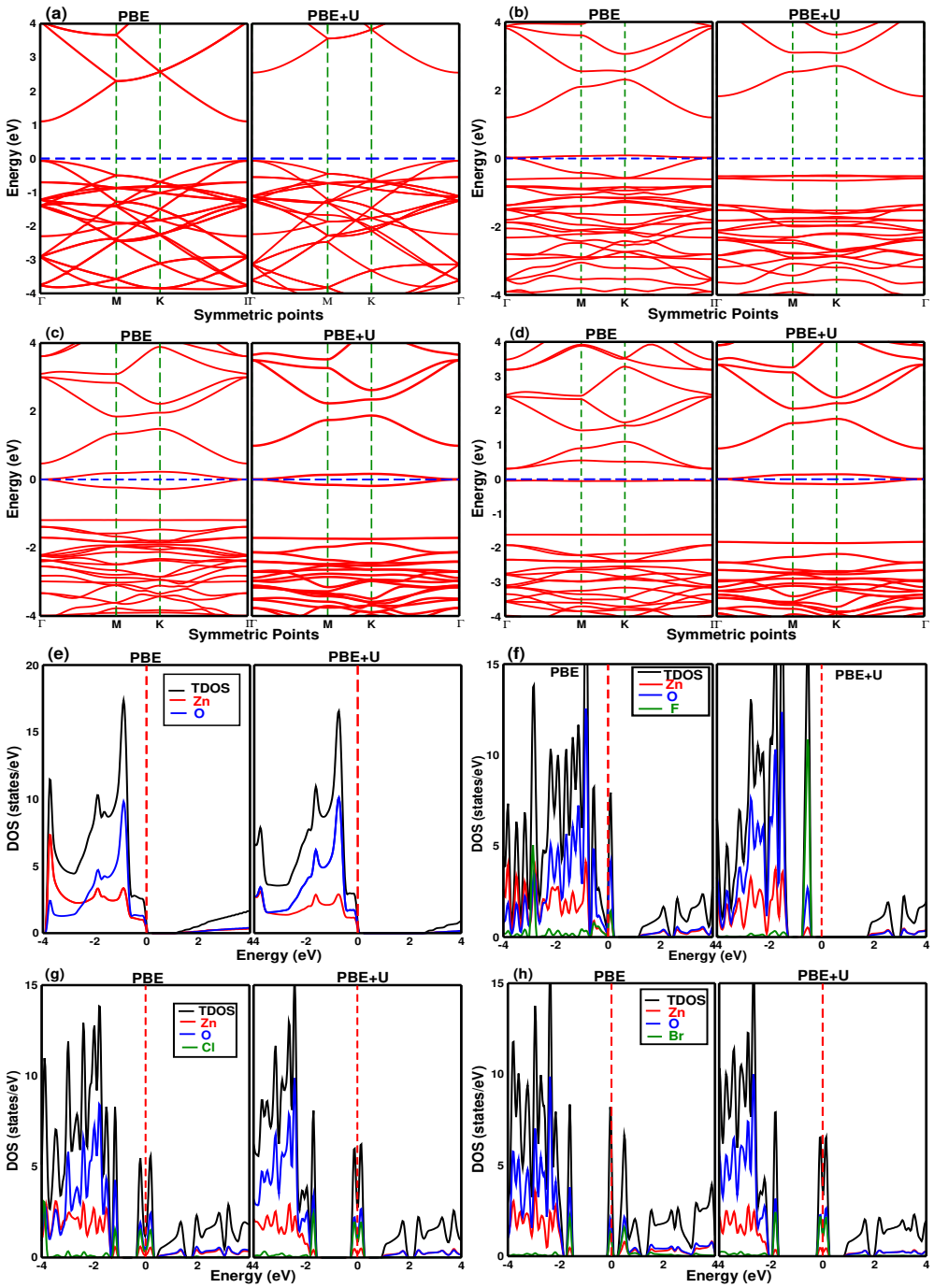

FIGURE 2. Band structures (a-d) and DoS (e-f) of: Pristine ZnO, F-doped ZnO, Cl-doped ZnO, and Br-doped ZnO.

undoped and halogen doped ZnO. Figure 3(a) is the spin polarized density of state for pristine ZnO, which is obtained by employing PBE and PBE+U functional. In this graph, it is clearly seen that spin up and spin down are almost symmetric to each other that proves that ZnO is non-magnetic. Nonetheless, spin polarized DoS and PDoS of halogen Doped ZnO is not symmetric. Spin polarized DoS for F-ZnO in figure 3(b) is asymmetric while applying both the functional. Similarly, Figure 4 (a) shows the spin polarized DoS for Cl-ZnO and 4 (b) represent the spin up and spin down of Br-ZnO. The spin up and spin down for both the system are not symmetric, which suggest that both the compounds are magnetic in nature. Moreover, these asymmetric nature is seen due

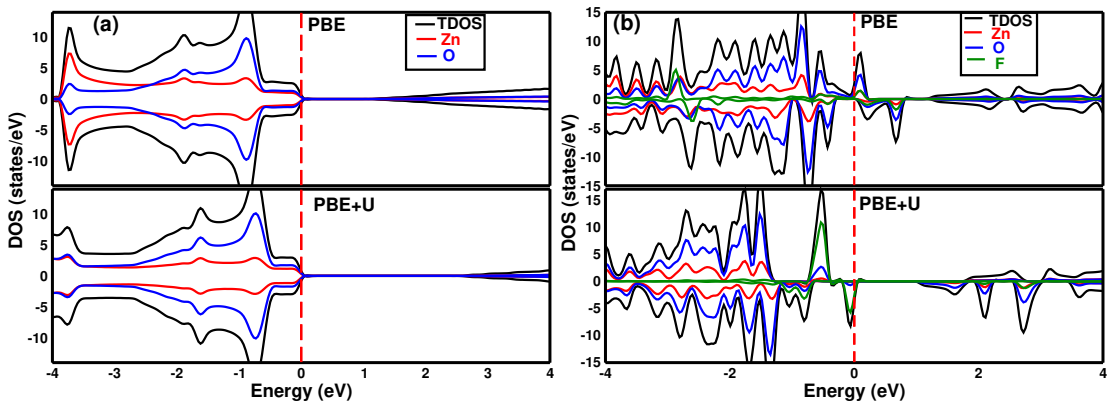

FIGURE 3. Spin polarized DOS: (a) Pristine ZnO, (b) F-doped ZnO

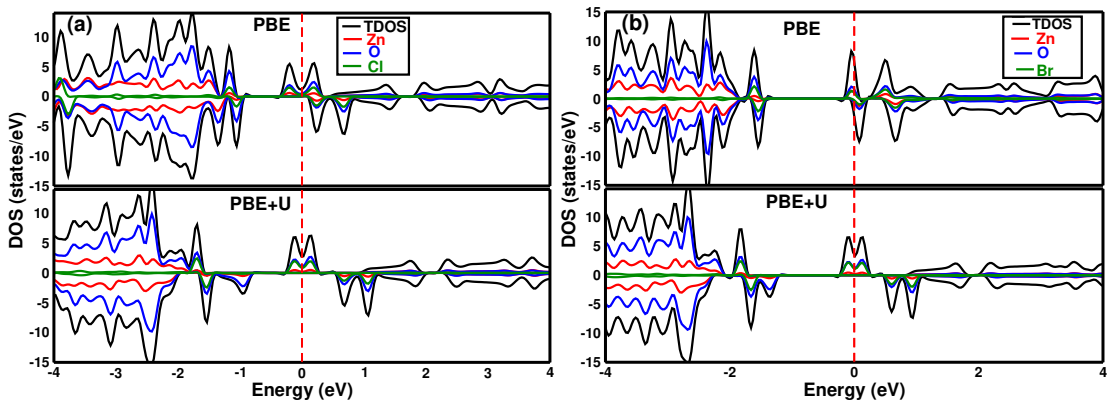

FIGURE 4. Spin polarized DoS: (a) Cl-doped ZnO, (b) Br-doped ZnO

to the unpaired electrons in the atom. Also, calculating the magnetic moment, we found the magnetic moment of 1.02 μB and 2.98 μB for F-ZnO, 1 μB and 1μB for Cl-ZnO and 1 μB and 1 μB for Br-ZnO, while applying PBE and PBE+U functional respectively. So, on the basis of these results, it can be concluded that halogen doped ZnO behaves like a magnetic materials.

CONCLUSION

In this work, we have studied the structural, electronic, and magnetic properties of undoped and halogen-doped ZnO monolayers by employing DFT using VASP computational tool. The formation energy and ground state energy represent that the systems are structurally stable. On the other hand, band gap of pure ZnO was found to be 1.67 eV and 2.61 eV while applying PBE and PBE+U functional, respectively. However, when halogen atoms are doped in ZnO, we found that the band gap is sharply decreased. Thus, calculated band gaps were found to be almost 0 eV for all the functional. Although, the bands of these systems crossed the Fermi level, bands in the conduction band and valance band do not overlap with each other. So, this implies that system under consideration behaves like a semimetallic material. Likewise, on computing the magnetic moment of these system, we found that the magnetic moment of pristine ZnO is 0 μB on applying PBE and PBE+U functional. Additionally, the magnetic moments of 1.02 μB & 2.98 μB for F-ZnO, 1.0 μB & 1.0 μB for Cl-ZnO and Br-ZnO were obtained. These results suggest that halogen-doped ZnO is semimetallic according to band structure calculations and magnetic materials according to density of states and partial density of states studies. As a result, halogen -doped ZnO, which has a conducting spin channel, may hold great promise for use in next-generation spintronic nanodevices.

ACKNOWLEDGEMENTS

The authors would like to thank the International Science Program (ISP), Uppsala University, Sweden, for supporting the Atmospheric and Material Science Research

Group at the Department of Physics, Amrit Campus, through NEP01, to conduct the computational work.

DATA AVAILABILITY

The data that are used to create figures and tables are available upon request to the corresponding author.

DECLARATIONS AND CONFLICT OF INTEREST

There is no known conflict of interest by the authors.

EDITORS' NOTE

This manuscript was rigorously peer-reviewed and subsequently accepted for inclusion in the special issue of the Journal of Nepal Physical Society (JNPS) after it was submitted to the Association of Nepali Physicists in America (ANPA) Conference 2024.

REFERENCES

1. K. S. Novoselov, A. Mishchenko, A. Carvalho, and A. Castro Neto, "2d materials and van der waals heterostructures," Science **353**, aac9439 (2016).
2. J. Jiang, T. Xu, J. Lu, L. Sun, and Z. Ni, "Defect engineering in 2d materials: precise manipulation and improved functionalities," Research (2019).
3. S. Das, A. Sebastian, E. Pop, C. J. McClellan, A. D. Franklin, T. Grasser, T. Knobloch, Y. Illarionov, A. V. Penumatcha, J. Appenzeller, *et al.*, "Transistors based on two-dimensional materials for future integrated circuits," Nature Electronics **4**, 786–799 (2021).
4. D. Berman, L. I. Farfan-Cabrera, A. Rosenkranz, and A. Erdemir, "2d materials for durable and sustainable electric vehicles," Nature Reviews Materials , 1–3 (2024).
5. D. Akinwande, C. J. Brennan, J. S. Bunch, P. Egberts, J. R. Felts, H. Gao, R. Huang, J.-S. Kim, T. Li, Y. Li, *et al.*, "A review on mechanics and mechanical properties of 2d materials—graphene and beyond," Extreme Mechanics Letters **13**, 42–77 (2017).
6. F. Withers, O. Del Pozo-Zamudio, A. Mishchenko, A. P. Rooney, A. Gholinia, K. Watanabe, T. Taniguchi, S. J. Haigh, A. Geim, A. Tartakovskii, *et al.*, "Light-emitting diodes by band-structure engineering in van der waals heterostructures," Nature materials **14**, 301–306 (2015).
7. Z. Sun, A. Martinez, and F. Wang, "Optical modulators with 2d layered materials," Nature Photonics **10**, 227–238 (2016).
8. M. Long, P. Wang, H. Fang, and W. Hu, "Progress, challenges, and opportunities for 2d material based photodetectors," Advanced Functional Materials **29**, 1803807 (2019).
9. Y. Liu, X. Duan, Y. Huang, and X. Duan, "Two-dimensional transistors beyond graphene and tmdcs," Chemical Society Reviews **47**, 6388–6409 (2018).
10. Y. Liu, N. O. Weiss, X. Duan, H.-C. Cheng, Y. Huang, and X. Duan, "Van der waals heterostructures and devices," Nature Reviews Materials **1**, 1–17 (2016).
11. S. Vaziri, *Complementary-metal Oxide Semiconductor (CMOS)*, Ph.D. thesis, California State University, Fresno (1985).
12. M. Rostami Osanloo, *The Dielectric Properties of Two-dimensional Materials and Their Applications in Electronic Devices: a First-principles Study*, Ph.D. thesis (2022).
13. C. Karthikeyan, P. Arunachalam, K. Ramachandran, A. M. Al-Mayouf, and S. Karuppuchamy, "Recent advances in semiconductor metal oxides with enhanced methods for solar photocatalytic applications," Journal of alloys and compounds **828**, 154281 (2020).
14. S. T. Tan, B. Chen, X. Sun, W. Fan, H. S. Kwok, X. Zhang, and S. Chua, "Blueshift of optical band gap in zno thin films grown by metal-organic chemical-vapor deposition," Journal of Applied Physics **98** (2005).
15. J. Lu, Z. Ye, Y. Zeng, L. Zhu, L. Wang, J. Yuan, B. Zhao, and Q. Liang, "Structural, optical, and electrical properties of (zn, al) o films over a wide range of compositions," Journal of Applied Physics **100** (2006).
16. H. Q. Ta, L. Zhao, D. Pohl, J. Pang, B. Trzebicka, B. Rellinghaus, D. Pribat, T. Gemming, Z. Liu, A. Bachmatiuk, *et al.*, "Graphene-like zno: A mini review," Crystals **6**, 100 (2016).
17. A. Chizhov, M. Rumyantseva, and A. Gaskov, "Light activation of nanocrystalline metal oxides for gas sensing: Principles, achievements, challenges," Nanomaterials **11**, 892 (2021).
18. M. Que, C. Lin, J. Sun, L. Chen, X. Sun, and Y. Sun, "Progress in zno nanosensors," Sensors **21**, 5502 (2021).
19. S. A. Patil, P. B. Jagdale, A. Singh, R. V. Singh, Z. Khan, A. K. Samal, and M. Saxena, "2d zinc oxide–synthesis, methodologies, reaction mechanism, and applications," Small **19**, 2206063 (2023).
20. Y. Xia, B. Wang, J. Zhang, Y. Feng, B. Li, X. Ren, H. Tian, J. Xu, W. Ho, H. Xu, *et al.*, "Hole doping in epitaxial mose2 monolayer by nitrogen plasma treatment," 2D Materials **5**, 041005 (2018).
21. G. Paudel, M. Nepal, S. Aryal, A. Devkota, and H. Neupane, "Effect of water adsorption on bilayer h-bn: First-principles study," Journal of Nepal Physical Society **9**, 56–62 (2023).
22. M. Nepal, G. Paudel, S. Aryal, A. Devkota, and H. K. Neupane, "Adsorption of water on vacancy defective h-bn bilayer at b and n sites: First-principles calculation," BIBECHANA **21**, 129–141 (2024).
23. H. M. R. Faruque, K. Hosen, A. J. Islam, and M. S. Islam, "Halogen doped electronic properties of 2d zno: A first principles study," in *2019 5th International Conference on Advances in Electrical Engineering (ICAEE)* (IEEE, 2019) pp. 727–731.
24. S. Ghosh, S. S. Yamijala, S. K. Pati, and C. Rao, "The interaction of halogen molecules with swnts and graphene," RSC advances **2**, 1181–1188 (2012).
25. A. Slassi, M. Hammi, Z. Oumekloul, A. Nid-bahami, M. Arejdal, Y. Ziat, and O. El Rhazouani, "Effect of halogens doping on transparent conducting properties of sno 2 rutile: An ab initio investigation," Optical and Quantum Electronics **50**, 1–13 (2018).
26. M. Ma, G. Liu, Z. Yang, and G. Zhang, "First-principles calculations of pb2+ adsorption by halogen-doped sns2," Physica B: Condensed Matter , 416054 (2024).
27. W. Zheng, X. Liu, J. Xie, G. Lu, and J. Zhang, "Emerging van der waals junctions based on tmds materials for advanced gas sensors," Coordination Chemistry Reviews **447**, 214151 (2021).
28. J. Hafner, "Ab-initio simulations of materials using vasp: Density-functional theory and beyond," Journal of computational chemistry **29**, 2044–2078 (2008).
29. C. Fonseca Guerra, J. Snijders, G. t. Te Velde, and E. J. Baerends, "Towards an order-n dft method," Theoretical Chemistry Accounts **99**, 391–403 (1998).
30. J. P. Perdew, K. Burke, and M. Ernzerhof, "Generalized gradient approximation made simple," Physical review letters **77**, 3865 (1996).
31. J. Heyd, G. E. Scuseria, and M. Ernzerhof, "Hybrid functionals based on a screened coulomb potential," The Journal of chemical physics **118**, 8207–8215 (2003).

32. R. M. Sheetz, I. Ponomareva, E. Richter, A. N. Andriotis, and M. Menon, "Defect-induced optical absorption in the visible range in zno nanowires," Physical Review B—Condensed Matter and Materials Physics **80**, 195314 (2009).
33. X. Ma, Y. Wu, Y. Lv, and Y. Zhu, "Correlation effects on lattice relaxation and electronic structure of zno within the gga+ u formalism," The Journal of Physical Chemistry C **117**, 26029–26039 (2013).
34. H.-C. Wu, H.-H. Chen, and Y.-R. Zhu, "Effects of al-impurity type on formation energy, crystal structure, electronic structure, and optical properties of zno by using density functional theory and the hubbard-u method," Materials **9**, 647 (2016).
35. K. Harun, N. A. Salleh, B. Deghfel, M. K. Yaakob, and A. A. Mohamad, "Dft+ u calculations for electronic, structural, and optical properties of zno wurtzite structure: A review," Results in Physics **16**, 102829 (2020).
36. A. Majid, W. Akram, and A. Dar, "Dft study of electronic and structural properties of sm: Gan," Computational materials science **88**, 71–75 (2014).
37. V. Wang, N. Xu, J.-C. Liu, G. Tang, and W.-T. Geng, "Vaspkit: A user-friendly interface facilitating high-throughput computing and analysis using vasp code," Computer Physics Communications **267**, 108033 (2021).
38. V. Wang, N. Xu, J. C. Liu, G. Tang, and W.-T. Geng, "Vaspkit: a pre-and post-processing program for vasp code," arXiv preprint arXiv:1908.08269 (2019).
39. K. Momma and F. Izumi, "Vesta: a three-dimensional visualization system for electronic and structural analysis," Journal of Applied crystallography **41**, 653–658 (2008).
40. K. Momma and F. Izumi, "Vesta 3 for three-dimensional visualization of crystal, volumetric and morphology data," Journal of applied crystallography **44**, 1272–1276 (2011).
41. Y. Mao, J. Zhong, and Y. Chen, "First principles study of the band structure and dielectric function of (6, 6) single-walled zinc oxide nanotube," Physica E: Low-dimensional Systems and Nanostructures **40**, 499–502 (2008).
42. R. Vidya, P. Ravindran, H. Fjellvåg, B. Svensson, E. Monakhov, M. Ganchenkova, and R. M. Nieminen, "Energetics of intrinsic defects and their complexes in zno investigated by density functional calculations," Physical Review B **83**, 045206 (2011).
43. T. Dietl and H. Ohno, "Dilute ferromagnetic semiconductors: Physics and spintronic structures," Reviews of Modern Physics **86**, 187 (2014).
44. D. D. Awschalom and M. E. Flatté, "Challenges for semiconductor spintronics," Nature physics **3**, 153–159 (2007).